

# A comparison study of applying metallic coating on SiC particles for manufacturing of cast aluminum matrix composites

R. Taherzadeh Mousavian<sup>1</sup> & S. R. Damadi<sup>2</sup> & R. Azari Khosroshahi<sup>2</sup> & D. Brabazon<sup>3</sup> & M. Mohammadpour<sup>2</sup>

\* R.TaherzadehMousavian rtaher1898@gmail.com; r\_taherzadeh@sut.ac.ir

<sup>1</sup> Young Researchers and Elite Club, Ilkhchi Branch, Islamic Azad University, Ilkhchi, Iran

<sup>2</sup> Faculty of Materials Engineering, Sahand University of Technology, Tabriz, Iran

<sup>3</sup> Advanced Processing Technology Research Centre, School of Mechanical & Manufacturing Engineering, Dublin City University, Dublin 9, Ireland

## Abstract

Ceramic particles typically do not have a sufficiently high wettability for incorporation into molten metal during aluminum matrix composite manufacturing. Metallic coatings on ceramic particles could improve their wettability by the molten aluminum and hence provide a better bonding between the reinforcement and matrix. In this study, micrometer-sized SiC particles were coated by copper, nickel, and cobalt metallic layers using electroless deposition method. These metallic layers were produced separately prior to ceramic incorporation into molten pure aluminum, in order to compare their effects on the microstructure and mechanical properties of the produced composites. The experimental results showed that copper was the most effective and nickel the least effective of these coating metals for incorporation of the SiC particles into the molten aluminum. It was additionally found that the composite, which contained the copper coated SiC particles, produced the highest microhardness and tensile strength, while that fabricated with the cobalt-coated SiC particles produced the lowest microhardness and tensile strength.

## Keywords

Metallic coating · Aluminum matrix composite · Casting · Electroless deposition

## 1 Introduction

Aluminum metal matrix composites (AMMCs) have gained significant attention in recent years. This is primarily due to their lightweight, low coefficient of thermal expansion (CTE), machinability, and improved mechanical properties, such as increased 0.2 % yield strength (YS), ultimate tensile strength (UTS), and hardness [1-5]. Due to these advantages, they are used in aerospace industries (airframe and aerospace components), automobile industries (engine pistons), and electronic components [6-11].

Stir casting (vortex technique) is generally accepted commercially as a low-cost method for manufacturing of AMMCs. Its advantages lie in its simplicity, flexibility, and applicability to large volume production. This process allows very large-sized components to be fabricated. However, methods of achieving the following in stir casting must be considered: (i) no adverse chemical reaction between the reinforcement material and matrix alloy, (ii) no or very low porosity in the cast AMMCs, (iii) wettability between the two main phases, and (iv) achieving a uniform distribution of the reinforcement material [12-17].

Some of the methods used to achieve these goals during stir casting of AMMCs are the modification of the alloy composition, coating or specific treatments to the reinforcements, and control of the process parameters (stirring temperature, time, etc.) [16, 18-20]. Among these, coating of the reinforcement is a successful technique used to promote wetting of the particles by aluminum through decreasing the surface energy of the solid-liquid ( $\sigma_{sl}$ ). Metallic coatings of nickel or copper have been widely used to improve the wettability of carbon fibers and ceramic particles by molten aluminum alloys [16, 21-24]. The success of metallic coating layer for

incorporation of the ceramic particles into molten metal depends on the reaction tendency with molten metal and the melting temperature of metallic layer. It seems that a metal with a melting temperature close to that of the matrix material would not be a good choice in this regard. In fact, the metallic coating layer should not be immediately dissolved just after incorporation into molten metal, which this occurrence depends on the melting temperature of a metallic coating and its tendency for reaction with molten metal. The best condition in this regard is for this layer to remain around the particle after stirring and solidification of the matrix. The weight of metallic layer might also be an important parameter to control in order to aid further ceramic incorporation. From an economic viewpoint, Cu, Ni, and Co are metals that could be deposited via low-cost process of electroless deposition (ED), in comparison to expensive alternatives such as Au, Ag, Pt, and Pd. To the best of our knowledge, no attempt has been made to compare the operation of copper, nickel, and cobalt coating layers on the degree of incorporation of ceramic particles in a molten metal while using the same stir casting conditions to indicate which one has the above requirements as carrier of ceramic powders into the molten metal.

In this study, micrometer-sized SiC particles were coated with Cu, Ni, and Co using the ED method. The coated particles were then incorporated into the molten pure aluminum to assess their effects on the ceramic incorporation. The mechanical properties of the final composites were evaluated for comparison.

## 2 Experimental procedures

Aluminum ingot with 99.8 wt% commercial purity was used as a matrix. Table 1 tabulates the chemical composition of the used ingot obtained using an M5000 optical emission spectrometer. As can be seen, the amount of Si and Fe was almost negligible.

Micrometer-sized SiC particles with an average particle size of 80  $\mu\text{m}$  and 99.9 % purity were supplied (Shanghai Dinghan Chemical Co., Ltd. China) as the reinforcement of AMMCs. The morphology of the silicon carbide particles used in this study was shown in our previous studies [19, 20] using scanning electron microscopy (SEM) micrographs.

The preparation procedure of ED used for production of the metallic coating on SiC particles was also reported in these studies [19, 20]. Tables 2, 3, and 4 show the chemicals that were used for cobalt, nickel, and copper electroless coatings, respectively, as well as their concentrations. In addition, the amounts of pH and bath temperature are reported in these tables. Magnetic stirring speed was set at 400 rpm for all the baths.

Four sample types were fabricated in this study. Table 5 summarizes the four types of samples prepared. One gram of reinforcement powder from each sample was encapsulated carefully in an aluminum foil packet before the casting process in order to fabricate a composite with 3 wt%SiC ( $\approx 2.54$  vol.%SiC) as reinforcement. These packets

were preheated at 350  $^{\circ}\text{C}$  for 2 h for removing the moisture and impurities from the powders. The pure aluminum was heated to 680  $^{\circ}\text{C}$  within a bottom-pouring furnace. A graphite stirrer was placed below the surface of melt and rotated with a speed of 500 rpm, and simultaneously, argon with a high purity (99.9999 %) was used as a protective shroud on the melt surface. The packets were added to the vortex center, and the stirring was continued for 6 min. The composite slurry was poured into the preheated low-carbon steel mold (at 450  $^{\circ}\text{C}$ ). The schematic of the vortex-casting set-up was shown in detail in our previous study [4].

Microhardness test was conducted according to ASTM E384 using an applied load of 25 g for a 15-s duration. At least ten measurements were taken from fabricated samples. The tensile tests were performed at room temperature using an Instron-type testing machine operating at a constant rate of crosshead displacement, with an initial strain rate of  $2 \times 10^{-3} \text{ s}^{-1}$ . The YS, UTS, and ductility (percent elongation to break) were measured and averaged over three test samples. The dog-bone-shaped tensile specimens had a gauge size of 6 mm in diameter and 30 mm in length, according to ASTM B557M-10. Finally, SiC powders, which were coated with all three metals, were exposed to X-ray analysis (Bruker's D8 advance system, Germany) using Cu K $\alpha$  ( $\lambda=0.15405 \text{ nm}$ ) radiation to investigate the phase analysis after ED process. Microstructural investigations were performed using a scanning electron microscope (SEM, Cam Scan Mv2300, equipped with EDAX analysis) and an optical microscopy. An image analysis software (ImageJ, Gaithersburg, MD, USA) was used to determine the average thickness of the coating layer obtained by the SEM characterization from three different parts. For this purpose, the samples were polished and etched with

Keller's reagent (190 ml water, 5 ml HNO<sub>3</sub>, 3 ml HCl, and 2 ml HF). Finally, the incorporation percent of ceramic particles into the molten pure aluminum was examined using a graphical method, in which the full details of this method, which could quantitatively make a connection between the percentage of SiC incorporated within the solidified composite and the wettability of different coated particles, were published by Hashim et al. [25].

### 3 Results and discussion

Our previous studies [4, 18] indicated that uncoated silicon carbide particles could not be highly incorporated into the molten pure aluminum, meaning that a special process is necessary to improve the wettability of ceramic particles by molten metal. Figure 1 shows the microstructure of sample S<sub>1</sub>, in which uncoated SiC particles were used as reinforcement. As can be seen, the amount of ceramic particles is not considerable, and agglomerated particles were observed in some parts.

In order to improve the incorporation of these particles, metallic coatings of cobalt, nickel, and copper were used. Figure 2a shows the morphology of SiC powders coated by cobalt. The coating layer appears to be well adhered. It seems that even the edges of the surfaces were uniformly covered by cobalt layer. For evaluation of the coating uniformity, the coated ceramic particles were cold-pressed, and the uniformity was studied after breaking of the coated layers. By cold pressing the coated particles, it was found that a uniform coating of cobalt on the SiC particles was formed (see Fig. 2b). An average thickness of the coating layer was determined to be around 1.83 μm. XRD analysis of cobalt-coated SiC particles also shows the formation and detection of SiC and Co phases after the ED process (Fig. 2c), and point EDAX analysis (Fig. 2d) of the yellow-colored cross shown in Fig. 2a indicated the presence of Co, P, and Au elements. Au is detected due to the usage of gold coating, which was applied for SEM characterization. These analyses indicated the success of ED process for coating of Co-P layer on the SiC particles.

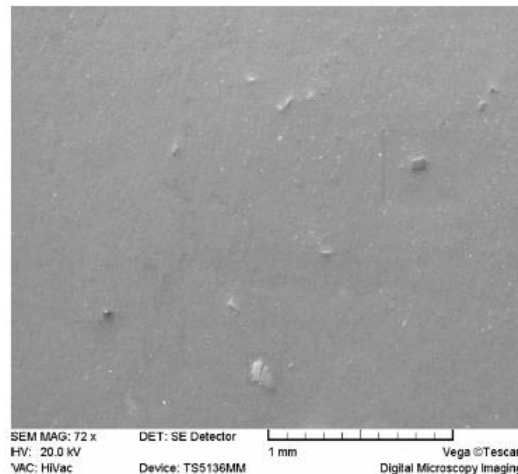


Fig. 1 The SEM microstructure of sample S<sub>1</sub>, in which uncoated SiC particles were incorporated as reinforcement

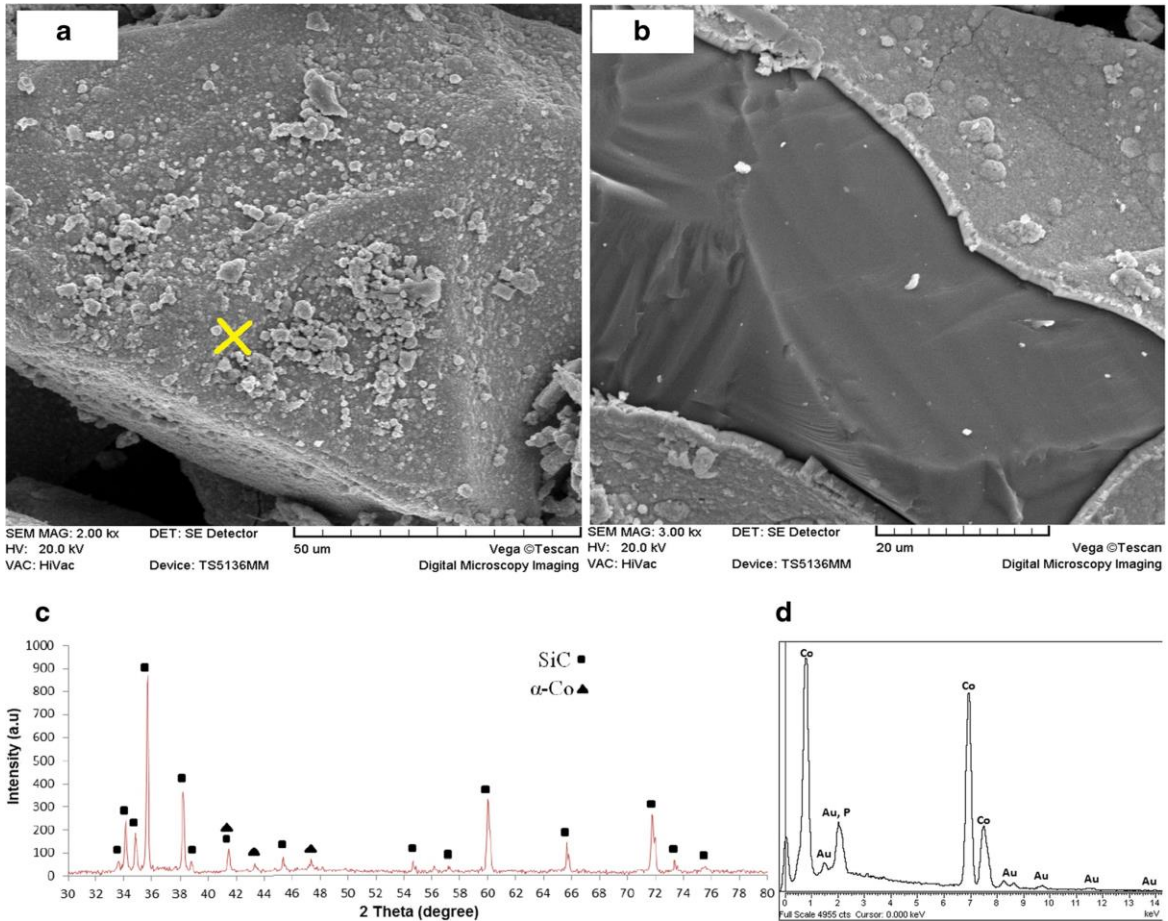


Fig. 2 The SEM morphology of Co-coated SiC particles a after ED process and b after cold pressing, c XRD analysis of Co-coated particles after ED, and d point-EDAX analysis of the yellow colored cross shown in a

These Co-coated SiC particles were carefully encapsulated in the aluminum foil and injected into the molten pure aluminum, as described earlier, to form sample S<sub>2</sub>. Figure 3 shows the SEM image of this sample microstructure as obtained after vortex casting. It is evident in the figure that the number of SiC particles is appreciable in respect to that of sample S<sub>1</sub>. For sample S<sub>2</sub>, a composite with a relatively uniform distribution of ceramic particles was obtained. The uniform distribution of the ceramic particles indicated in Fig. 3 shows that this method (ED process of cobalt) might be also useful to avoid ceramic particle agglomeration. The formation of gas pores could also be seen in the microstructure of sample S<sub>2</sub>, their formation of which is expected after 6 min stirring at 680 °C. Figure 4 shows a high magnification SEM micrograph of a SiC particle in sample S<sub>2</sub> where a fingerprint-like structure was formed around the SiC particles (white-colored parts). Both point and line EDAX analyses indicated that this structure is rich in cobalt, meaning that separation of cobalt layer from the ceramic particles occurred during incorporation and stirring at 680 °C. Point EDAX analysis (red-colored square) shows the presence of about 14 % atomic cobalt in this part. Based on the Al-Co phase diagram [26], Al<sub>9</sub>Co<sub>2</sub>, Al<sub>13</sub>Co<sub>4</sub>, and Al<sub>3</sub>Co are the phases, which could be formed via exothermic-nature reactions between cobalt with the molten aluminum [27, 28]. It seems that atomic percent of cobalt versus aluminum obtained in this study is close to Al<sub>9</sub>Co<sub>2</sub> phase with monoclinic structure [26].

The microstructure of nickel-coated SiC particles is shown in Fig. 5. This coating quality was obtained in our previous study [20] as the best condition, which could be prepared using the mentioned bath (see Table 3).

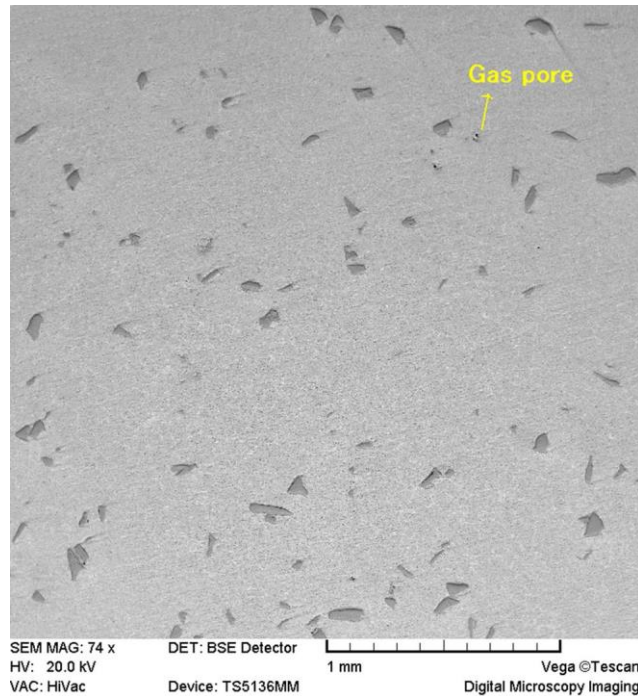


Fig. 3 The low-magnification SEM microstructure of sample  $S_2$  after casting

From Fig. 5a (the morphology of Ni coated SiC particles) and b (cold-pressed Ni coated SiC particles), it seems that the nickel layer almost covered all the ceramics surfaces with a relative uniformity. An average thickness of about  $1.02 \mu\text{m}$  was obtained for the Ni-P coating layer (see Fig. 5b). It is important to note that Si was detected beside Ni and P after point EDAX analysis (Fig. 5c) of the yellow-colored cross shown in Fig. 5a; this element had not been detected for Co-coated SiC particles. This means that the thickness of the coating layer might be effective on the detection of silicon, as it was found that a lower amount of average thickness was obtained for nickel ( $1.02 \mu\text{m}$ ) compared with that of cobalt ( $1.83 \mu\text{m}$ ). The XRD result (Fig. 5d) also shows the formation of intensive SiC peaks as well as reveal Ni and P peaks after ED process. Figure 6a shows the microstructure of as-cast sample  $S_3$  indicating the considerable presence of SiC particles that incorporated into the molten aluminum. However, it seems that, irrespective of a relative good distribution of ceramic particles, the amount of reinforcement is lower than that of the sample  $S_2$ . A high-magnification SEM image (see Fig. 6b) for sample  $S_3$  indicated that nickel was separated from the SiC particles like cobalt, entered in the molten Al, and might react with the matrix to form intermetallic phases, which Rajan et al. [29] indicated that the nature of reaction between the molten aluminum with nickel coating layer is exothermic. Point EDAX analysis of white-colored parts indicated the presence of only 5 at.% of nickel; this amount is lower than that obtained after point EDAX analysis of white-colored parts (red-colored cross shown in Fig. 6b) of sample  $S_2$ . Figure 7 is related to a line EDAX analysis related to sample  $S_3$ . This figure indicates a remain of a part of nickel layer on the SiC particles after grinding and polishing, suggesting that nickel layer might be strongly adhered to the particles after ED process in some parts. In fact, this figure shows that the separation of the coating layer at  $680^\circ\text{C}$  for 6 min stirring is not peremptory, and based on the coating adhesion to the ceramic surface, it is possible to observe a partial layer on the ceramic particle after casting and solidification.

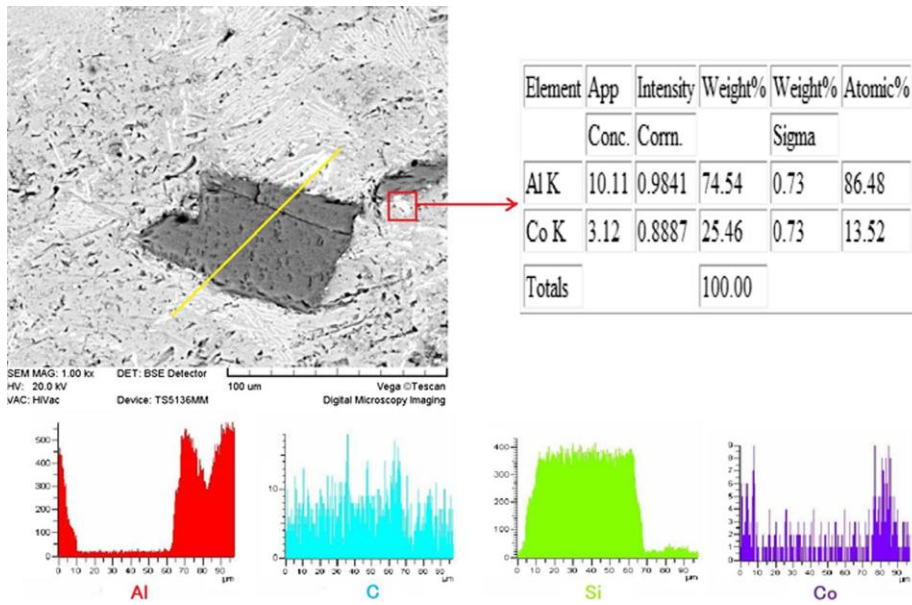


Fig. 4 The high-magnification SEM microstructure of sample S<sub>2</sub> as well as point and line EDAX analyses from the shown regions

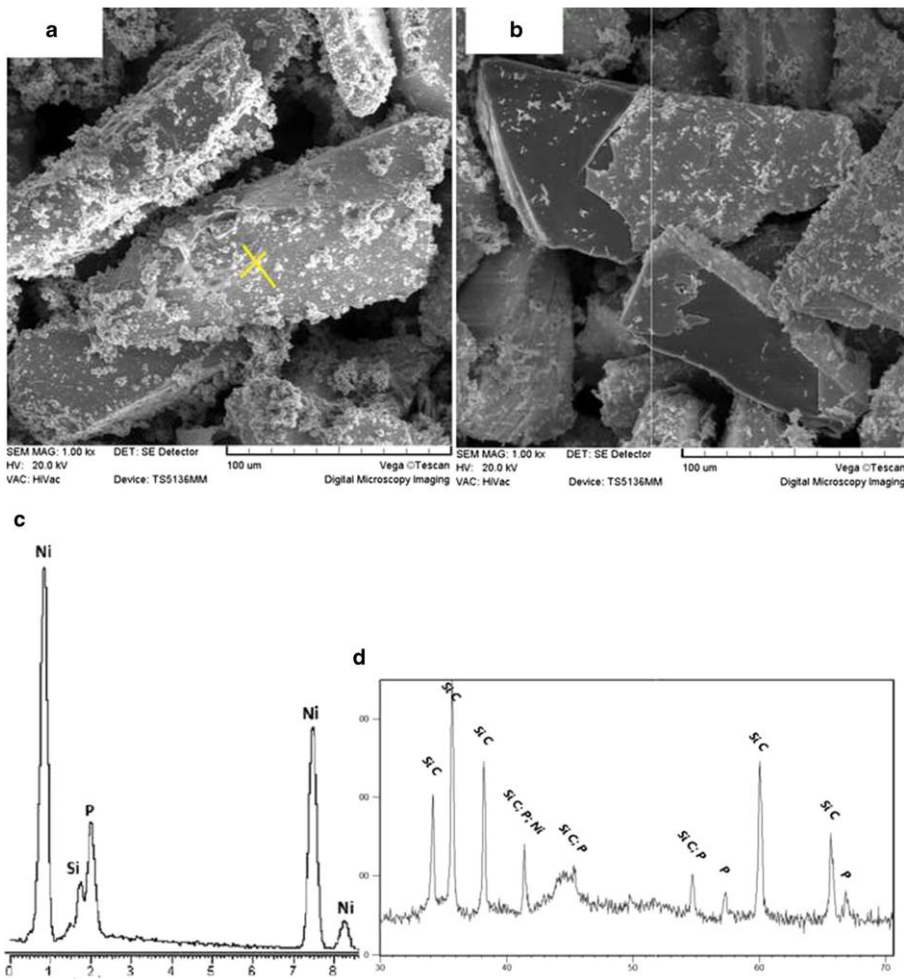


Fig. 5 The SEM morphology of Ni-coated SiC particles a after ED process and b after cold pressing, c point EDAX analysis of the yellow colored cross shown in a, and d XRD analysis of Ni-coated particles after ED

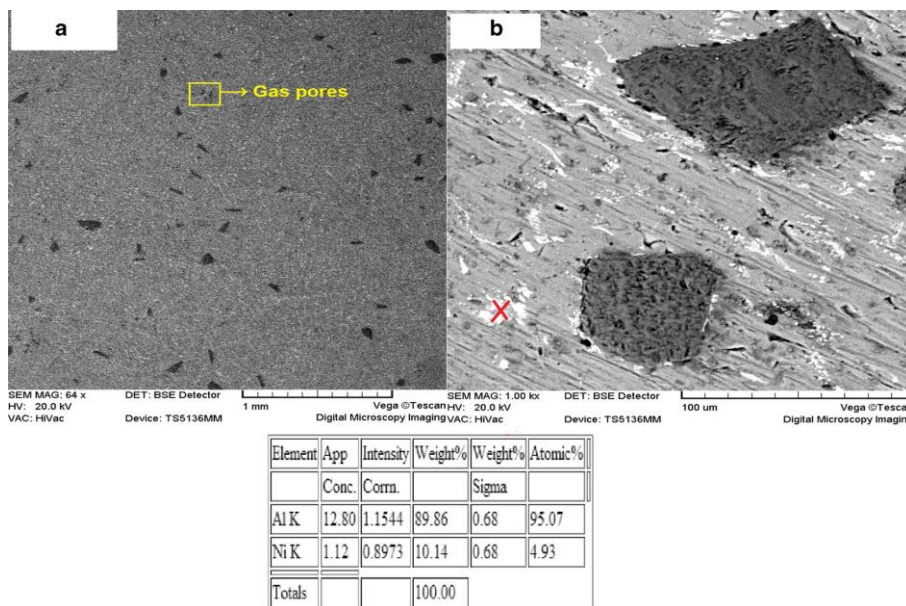


Fig. 6 The SEM microstructures of sample  $S_3$  as well as point EDAX analysis of the red colored cross: a low magnification and b high magnification

However, as Figs. 2b and 5b show, the metallic coatings on ceramic particles do not have sufficient flexibility and adhesion, and after cold pressing, they were broken. This means that the shear stress caused by vortex formation at 680 °C could separate the metallic coating during stirring. It should be noted that the tendency of the coating layer for dissolution and reaction with the molten aluminum could be another strong reason as well as the lack of enough flexibility and adhesion of the coating layer for separating from the reinforcement phase during liquid-state preparation of AMMCs. It was reported in the study of Rajan et al. [29] that the exothermic nature of possible reactions that might have occurred between the coating layers with the molten aluminum increases the mobility of coating layer that may lead to its sweeping away from the ceramic interface. This occurrence might reduce the potential of metallic layer regarding the improvement of ceramic particles incorporation. It should be noted that the main benefit of the ED process in this study was to maximize the ceramics incorporation into the molten metal when they passed through the surface of the aluminum melt and entered the vortex. The second benefit of using ED process is to fabricate a hybrid composite material with two kinds of the reinforcement as the metallic layer could react with molten metal and form some phases, which the mechanical properties results indicated that these phases increased the strength of the composite.

Figure 8a shows the morphology of copper-coated SiC particles after the ED process. The bath parameters for copper coating were previously optimized in our previous study [19]. As can be seen from this figure, a relatively thick layer of copper was formed uniformly on the SiC particles. The uniformity of the coating could be observed in Fig. 8b, which the coated particles were cold-pressed. It was found that the average thickness of the copper coating layer is about 1.79  $\mu\text{m}$ , which is very close to that of cobalt. The results of XRD analysis (Fig. 8c) of the Cu-coated particles and point EDAX analysis (Fig. 8d) of the yellow-colored cross shown in Fig. 8a indicated the formation of copper and SiC after ED process without the detection of the other phases.

Figure 9a shows the microstructure of as-cast sample  $S_4$ , containing the SiC particles, which were covered by a copper layer. The incorporation of a wide number of ceramic particles is evident for this sample. However, it seems that the agglomeration of these particles occurred in some parts, in which this phenomenon is inevitable during the casting process. All the as-cast microstructures of the samples indicate that a secondary high-temperature process like extrusion or rolling might be needed after casting to decrease the amount of porosities and improve the distribution of reinforcement phase especially via separation of agglomerated particles.

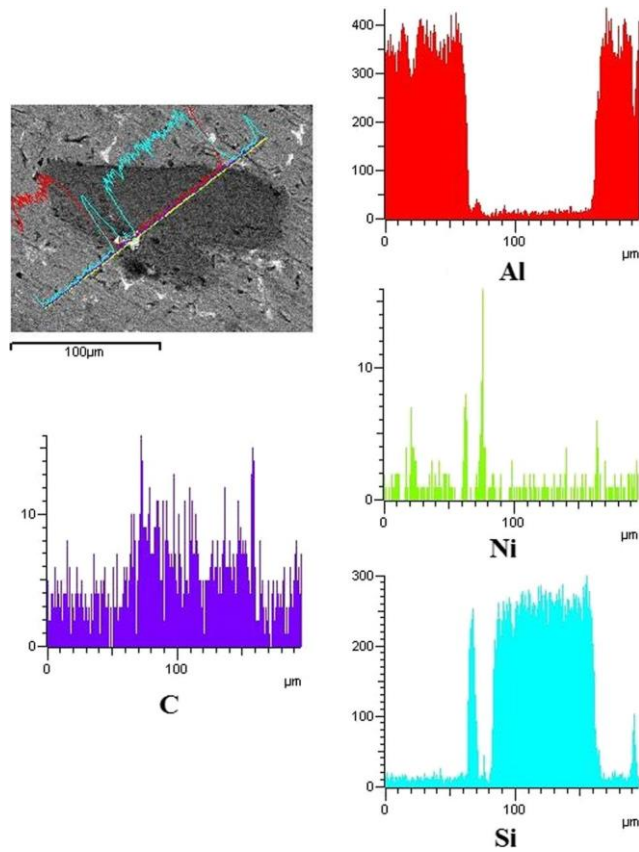


Fig. 7 Line EDAX analysis of sample  $S_3$

The formation of an Al-SiC interface with a good bonding is also observed for this sample from high-magnification SEM image (see. Fig. 9b). Such a defect-less bonding could not be observed in the microstructure of the previous samples. Many authors also reported that a strong bonding would be formed between ceramic particles and metal matrix if copper is coated on the surface of ceramic particles [30, 31]. Line EDAX analysis for sample  $S_4$  indicated that white-colored areas are related to the presence of copper in the matrix of aluminum. It was reported [29] that copper dissolution in the molten aluminum has an endothermic nature, which helped the coating layer to be retained around the ceramic surface. This phenomenon could lead to the formation of a more strong bonding between Al and SiC. In addition, the retention of the coating layer could increase the incorporation percentage of ceramic particles.

As mentioned, the presence of a metallic layer provides improved wettability of micrometer-sized ceramic particles. Figure 10 shows a schematic of casting process when uncoated and metal-coated ceramic particles were injected into the molten aluminum at 680 °C after 6 min stirring. This schematic shows the usage of an aluminum foil, a ceramic plug in the bottom of crucible, and a graphite stirrer for casting process. As can be seen, a layer oxide film is always present on the surface of the melt, especially when argon is not used. As this figure shows, the uncoated SiC particles could not be entered into the molten metal due to the poor wetting by the matrix. Even 6 min stirring was not effective in order to trap these particles via the vortex casting method. The schematics at the bottom of Fig. 10 indicate the considerable effect of metallic coating on the ceramic incorporation. The main reason, which was responsible for this, was a sharp reduction of wetting contact angle ( $\alpha$ ) due to the applied metallic coating. The extent of wetting on a solid-liquid interface, such as molten aluminum in contact with SiC particles, can be described using the Young-Dupre equation [16]:

$$\gamma_{LV} \cos \alpha = \gamma_{SV} - \gamma_{SL} \quad \delta l p$$

where  $\gamma$  denotes surface tension, and the subscripts L, S, and V denote liquid, solid, and vapor.  $\alpha$  is the contact angle



between solid and liquid (see Fig. 10). Contact angle is a metric for the degree of wetting. A liquid is considered to wet a solid for  $\cos\alpha > 0$ , or when  $\sigma_{sv} > \sigma_{sl}$ . In that situation, the solid would prefer to form interfaces with the liquid over the vapor, since coverage by a liquid would lower the free energy of the solid by  $(\sigma_{sv} - \sigma_{sl})dA$  [16]. In fact, by applying a metallic coating on SiC particles, a metal/metal interaction would occur when the particles pass through the surface of the melt. This would decrease the  $\sigma_{sl}$ , and therefore, a lower amount of contact angle would be obtained. Drew and his co-workers [21, 32, 33] indicated that using nickel and copper on the SiC particles would decrease the wetting contact angle of the liquid drop on the ceramic substrate from about 120 to  $<40^\circ$  after about 6 min.

Figure 11 shows the effect of cobalt, nickel, and copper coatings on the ceramic incorporation percentage. As can be seen, copper, cobalt, and nickel are effective as regards ceramic incorporation, respectively. This ability for improving the ceramic incorporation might be related to many factors such as the weight and melting temperature of coating metal, the tendency for reaction and dissolution in the matrix, and the thickness of the coating layer. As mentioned, the exothermic reactions increase the mobility of the coating layers and might reduce the incorporation percentage of ceramic particles. It is obvious from Fig. 11 that copper with endothermic reactions with molten aluminum causes the sample S<sub>4</sub> to have the highest amount of ceramic incorporation. In addition, the thickness value of the nickel layer is lower than that of the copper and cobalt layers and that this matter might also cause the sample S<sub>3</sub> to have the lowest amount of ceramic incorporation percentage.

During the solidification of a composite, internal stresses are developed around the ceramics due to a difference in the CTE of the aluminum and the SiC particle, and they are relieved by formation and movement of dislocations [34-36]. In order to evaluate the effect of the metallic coatings on the mechanical properties of the fabricated samples, ten random points were selected within each sample for microhardness measurements (Vickers, 25 g load).

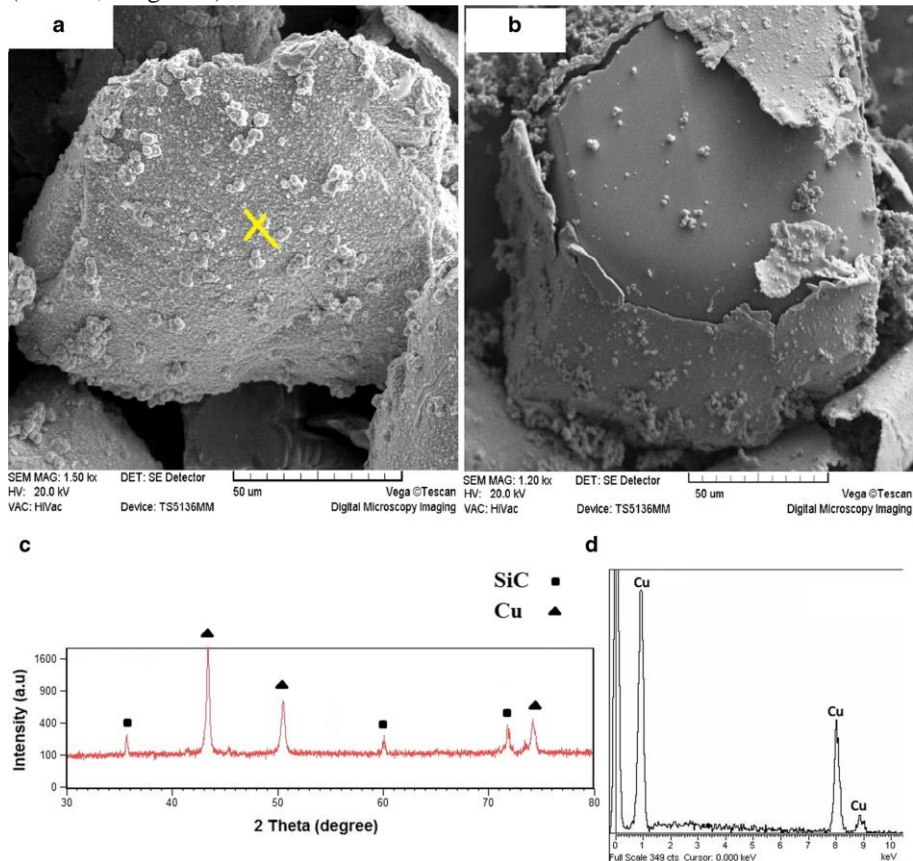


Fig. 8 The SEM morphology of Cu-coated SiC particles a after ED process and b after cold pressing, c XRD analysis of Cu-coated SiC particles after ED, and d point-EDAX analysis of the yellow colored cross shown in a

Table 6 shows the mechanical property values of the samples. As can be seen, sample S<sub>4</sub> was harder than the other samples, and the usage of metallic coating highly increased the microhardness value as just about 44 HV microhardness was obtained for sample S<sub>1</sub>. Sample S<sub>3</sub> that contains a lower amount of SiC particles was also revealed to be harder than sample S<sub>2</sub>, which might be due to the structure of intermetallic compounds, which were formed during stirring. It is very important to note that the amount of porosities was not considerable for all the samples, and it seems that this parameter was not effective on the microhardness values. Hence, the quantity of ceramic particles as well as intermetallic compounds formed during casting might be two important factors that affect the hardness of the composites. As can be seen, the usage of metallic coating also made a very intensive effect on the strength and ductility of the composites in respect to those of sample S<sub>1</sub>. Similar to the values of microhardness, the same trend seems to be obtained for YS and UTS values of the samples. The most important point, which could be drawn from Table 6, is the value of break strain (%) or ductility of sample S<sub>4</sub>. In fact, sample S<sub>4</sub> that contains Cu-coated SiC particles has a higher microhardness, YS, and UTS values, while a higher value of ductility was obtained for this sample in respect to those of samples S<sub>2</sub> and S<sub>3</sub>.

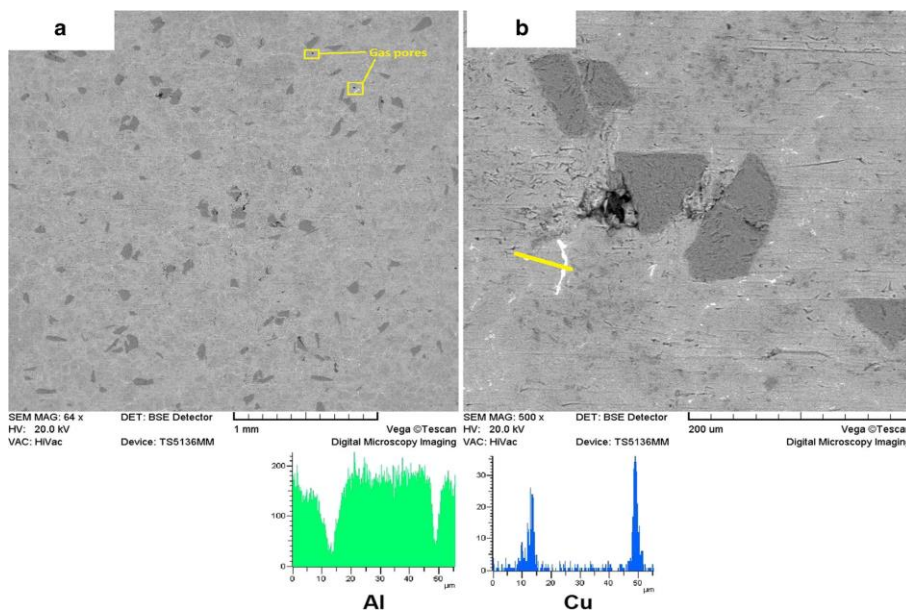


Fig. 9 The SEM microstructures of sample S<sub>4</sub> as well as line EDAX analysis from the shown region: a low magnification and b high magnification

This occurrence could be emanated from the formation of a better bonding at the ceramic/matrix interface for this sample (see Fig. 9b). Another possible reason is the possible difference in the nature and mechanical properties of intermetallic compounds, which might be formed due to the entrance of Cu, Co, and Ni to the matrix during stirring. It was also obtained that the samples containing metal-coated ceramic particles have a lower ductility amount mainly due to incorporation of a higher amount of ceramic particles, and sample S<sub>3</sub> has the lowest amount of ductility.

## 4 Conclusions

In this study, the behavior of cobalt, copper, and nickel coatings on the SiC particles were compared and studied using the same casting parameters to indicate which one is more suitable for ceramic incorporation. From the experimental results, the following conclusions could be drawn:

1. No crack formation and uncovered parts could be seen on the SiC particles for all the three metals. In addition, a uniform coating layer was revealed for all of them. However, a lower average thickness was

obtained for the Ni-P coating layer (1.02  $\mu\text{m}$ ) compared with that of copper (1.79  $\mu\text{m}$ ) and cobalt (1.83  $\mu\text{m}$ ).

- For a composite containing Cu-coated SiC particles, 98.8 % incorporation was obtained, while 84.6 and 71.2 incorporation percents were obtained for composites that contain Co-P and Ni-P coated SiC particles, respectively.
- The coating characteristics, in particular its thickness and its nature of reaction with the molten aluminum (exothermic or endothermic), affect the incorporation quantity of the ceramic reinforcement.
- The microhardness, YS, and UTS values of the composites were dependent on the amount of ceramic particles, the quality of bonding at the matrix/ceramics interfaces, and intermetallic compounds, which are formed during casting process. In comparison between the coating metals investigated, copper coatings produced the highest microhardness and strength, and cobalt the lowest. A higher value of ductility was obtained for the samples, which contained Cu-coated SiC particles, which may be a result of the formation of better bonding at the ceramic/matrix interface.

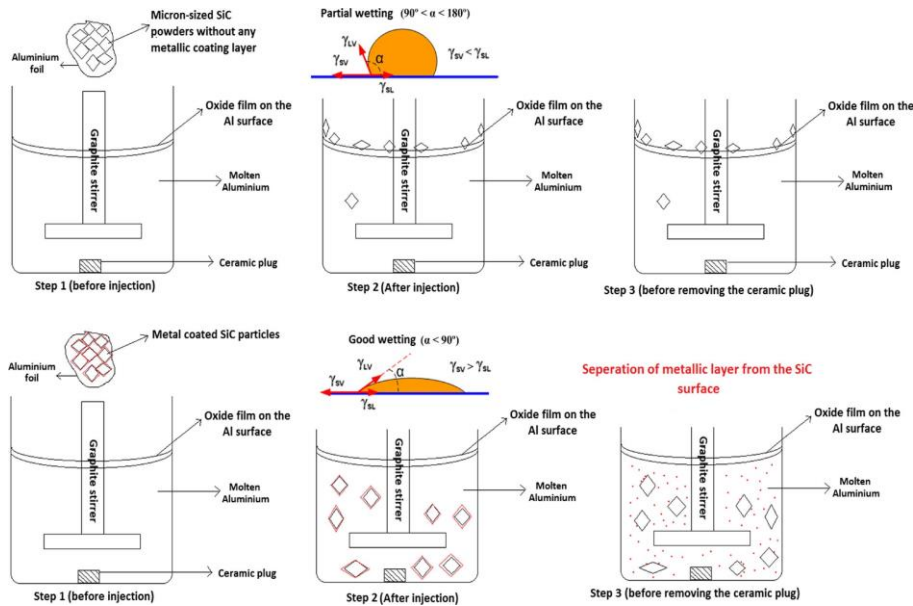


Fig. 10 Schematic of three steps in the casting process using as-received and metal-coated ceramic particles

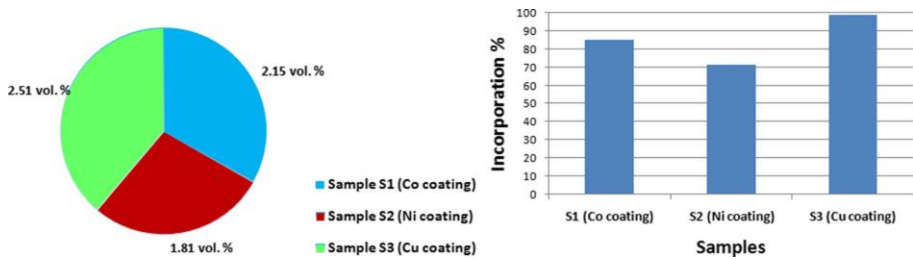


Fig. 11 The effect of metallic coatings on the SiC particle incorporation (%)

Table 6 The mechanical properties for the samples

Sample	UTS (MPa)	Break strain (%)	YS (MPa)	Hardness (HV)
Sample S <sub>1</sub>	85±6	13±2	57±4	44±3
Sample S <sub>2</sub> (Co)	131±6	6±2	89±4	117±6
Sample S <sub>3</sub> (Ni)	143±5	4±1	97±4	127±6
Sample S <sub>4</sub> (Cu)	154±8	8±2	109±5	136±6

## References

1. Srivatsan T (1996) Microstructure, tensile properties and fracture behaviour of  $\text{Al}_2\text{O}_3$  particulate-reinforced aluminium alloy metal matrix composites. *J Mater Sci* 31(5):1375-1388
2. Smagorinski M, Tsantrizos P (2000) Development of light composite materials with low coefficients of thermal expansion. *Mater Sci Technol* 16(7-8):853-861
3. Bhushan RK, Kumar S, Das S (2013) Fabrication and characterization of 7075 Al alloy reinforced with SiC particulates. *Int J Adv Manuf Technol* 65(5-8):611-624
4. Mohammadpour M, Khosroshahi RA, Mousavian RT, Brabazon D (2015) A novel method for incorporation of micron-sized SiC particles into molten pure aluminum utilizing a Co coating. *Metall Mater Trans B* 46(1):12-19
5. Dandekar CR, Shin YC (2013) Experimental evaluation of laser-assisted machining of silicon carbide particle-reinforced aluminum matrix composites. *Int J Adv Manuf Technol* 66(9-12):1603-1610
6. Roshan M, Mousavian TR, Ebrahimkhani H, Mosleh A (2013) Fabrication of Al-based composites reinforced with  $\text{Al}_2\text{O}_3$ - $\text{Tib}_2$  ceramic composite particulates using vortex-casting method. *J Min Metall B: Metall* 49(3):299-305
7. Ramanathan S (2013) Effect of silicon carbide volume fraction on the hot workability of 7075 aluminium-based metal-matrix composites. *Int J Adv Manuf Technol* 67(5-8):1711-1720
8. Valibeygloo N, Khosroshahi RA, Mousavian RT (2013) Microstructural and mechanical properties of Al-4.5 wt% Cu reinforced with alumina nanoparticles by stir casting method. *Int J Miner Metall Mater* 20(10):978-985
9. Canakci A, Arslan F (2012) Abrasive wear behaviour of B4C particle reinforced Al2024 MMCs. *Int J Adv Manuf Technol* 63(5-8): 785-795
10. Naher S, Brabazon D, Looney L (2007) Computational and experimental analysis of particulate distribution during Al-SiC MMC fabrication. *Compos A: Appl Sci Manuf* 38(3):719-729
11. Tzamtzis S, Barekar N, Hari Babu N, Patel J, Dhindaw B, Fan Z (2009) Processing of advanced Al/SiC particulate metal matrix composites under intensive shearing—a novel rheo-process. *Compos A: Appl Sci Manuf* 40(2):144-151
12. Naher S, Brabazon D, Looney L (2003) Simulation of the stir casting process. *J Mater Process Technol* 143:567-571
13. Hashim J, Looney L, Hashmi M (1999) Metal matrix composites: production by the stir casting method. *J Mater Process Technol* 92: 1-7
14. Rajan T, Pillai R, Pai B, Satyanarayana K, Rohatgi P (2007) Fabrication and characterisation of Al-7Si-0.35 Mg/fly ash metal matrix composites processed by different stir casting routes. *Compos Sci Technol* 67(15):3369-3377
15. Brabazon D, Browne D, Carr A (2002) Mechanical stir casting of aluminium alloys from the mushy state: process, microstructure and mechanical properties. *Mater Sci Eng A* 326(2):370-381
16. Hashim J, Looney L, Hashmi M (2001) The wettability of SiC particles by molten aluminium alloy. *J Mater Process Technol* 119(1):324-328
17. Prabu SB, Karunamoorthy L, Kathiresan S, Mohan B (2006) Influence of stirring speed and stirring time on distribution of particles in cast metal matrix composite. *J Mater Process Technol* 171(2):268-273
18. Mohammadpour M, Azari Khosroshahi R, Taherzadeh Mousavian R, Brabazon D (2014) Effect of interfacial-active elements addition on the incorporation of micron-sized SiC particles in molten pure aluminum. *Ceram Int* 40(6):8323-8332
19. Beigi Khosroshahi N, Azari Khosroshahi R, Taherzadeh Mousavian R, Brabazon D (2014) Electroless deposition (ED) of copper coating on micron-sized SiC particles. *Surf Eng* 30(10): 747-751
20. Beigi Khosroshahi N, Azari Khosroshahi R, Taherzadeh Mousavian R, Brabazon D (2014) Effect of electroless coating parameters and ceramic particle size on fabrication of a uniform Ni-P coating on SiC particles. *Ceram Int* 40(8):12149-12159
21. Leon C, Drew R (2002) The influence of nickel coating on the wettability of aluminum on ceramics. *Compos A: Appl Sci Manuf* 33(10):1429-1432
22. Bhav Singh B, Balasubramanian M (2009) Processing and properties of copper-coated carbon fibre reinforced aluminium alloy composites. *J Mater Process Technol* 209(4):2104-2110
23. Rams J, Urena A, Escalera M, Sánchez M (2007) Electroless nickel coated short carbon fibres in aluminium matrix composites. *Compos A: Appl Sci Manuf* 38(2):566-575
24. Urena A, Rams J, Escalera M, Sánchez M (2007) Effect of copper electroless coatings on the interaction between a molten Al-Si-Mg alloy and coated short carbon fibres. *Compos A: Appl Sci Manuf* 38(8):1947-1956
25. Hashim J, Looney L, Hashmi M (2001) The enhancement of wettability of SiC particles in cast aluminium matrix composites. *J Mater Process Technol* 119(1):329-335
26. McAlister A (1989) The Al-Co (aluminum-cobalt) system. *J Phase Equilib* 10(6):646-650
27. Gusak AM, Zaporozhets T, Lyashenko YO, Kornienko S, Pasichnyy M, Shirinyan A (2010) Diffusion-controlled solid state reactions: in alloys, thin-films, and nanosystems. Wiley-VCH Verlag GmbH and Co. KGaA, Boschstr. 12,69469, Weinheim, Germany John Wiley & Sons, p 105
28. Shevchenko M, Berezutskii V, Ivanov M, Kudin V, Sudavtsova V (2014) Thermodynamic properties of alloys of the Al-Co and Al-Co-Sc systems. *Russ J Phys Chem A* 88(5):729-734
29. Rajan T, Pillai R, Pai B (1998) Reinforcement coatings and interfaces in aluminium metal matrix composites. *J Mater Sci* 33(14): 3491-3503
30. Zhu S, Tang L, Cui Z, Wei Q, Yang X (2011) Preparation of copper-coated  $\beta$ -SiC nanoparticles by electroless plating. *Surf Coat Technol* 205(8):2985-2988
31. Yih P, Chung D (1996) Silicon carbide whisker copper-matrix composites fabricated by hot pressing copper coated whiskers. *J*

- Mater Sci 31(2):399-406
32. Leon C, Mendoza-Suarez G, Drew RA (2006) Wettability and spreading kinetics of molten aluminum on copper-coated ceramics. *J Mater Sci* 41(16):5081-5087
  33. Leon-Patino CA, Drew RA (2005) Role of metal interlayers in the infiltration of metal-ceramic composites. *Curr Opin Solid State Mater Sci* 9(4):211-218
  34. Ibrahim I, Mohamed F, Lavernia E (1991) Particulate reinforced metal matrix composites—a review. *J Mater Sci* 26(5):1137-1156
  35. Mortensen A, Gungor MN, Cornie J, Flemings M (1986) Alloy microstructures in cast metal matrix composites. *JOM* 38(3):30-35
  36. Asthana R (1998) Processing effects on the engineering properties of cast metal-matrix composites. *Adv Perform Mater* 5(3):213-255